Charge-Density-Wave Current Conversion in Submicron $NbSe_3$ Wires

O. C. Mantel, F. Chalin, C. Dekker, and H. S. J. van der Zant
Department of Applied Physics and DIMES, Delft University of Technology, Lorentzweg 1, 2628 CJ Delft, The Netherlands

Yu. I. Latyshev, B. Pannetier, and P. Monceau
Centre de Recherches sur les Très Basses Températures, associé à l'Université Joseph Fourier, CNRS, BP 166, 38042 Grenoble Cedex 9, France

(Received 29 June 1999)

We have studied the charge-density-wave (CDW) current conversion process in $NbSe_3$ wire structures of mesoscopic dimensions. A significant reduction of the phase-slip voltage associated with this conversion is observed if the spacing between current contacts is smaller than a few μm. This reduction cannot be explained with existing models of CDW current conversion. We suggest that single phase-slip events play a central role in micron-sized systems. The removal and addition of wave fronts may then become correlated in time.

PACS numbers: 72.15.Nj, 71.45.Lr, 73.23.–b

The sliding motion of charge-density waves (CDWs) causes remarkable electrical transport phenomena in conductors with a chainlike structure [1]. At the interface between a metallic contact and a CDW conductor, this sliding must inevitably be accompanied by injection of charge into the CDW condensate. According to current understanding, conversion occurs through strain-induced phase-slip processes, analogous to phase slip in narrow superconducting channels [2] and superfluids [3].

Sliding CDWs can be visualized as moving wave fronts that are coupled by elastic forces. The motion of these wave fronts causes a compression of the elastic CDW near one contact and a stretching near the other. Near contacts, phase slips can remove this strain [4,5]: a local amplitude defect is formed which grows across the whole sample cross section, so that one complete wave front is added or removed. The rate at which wave fronts are added is determined by the strain amplitude. The CDW strain profile has been studied by several techniques, including electromodulated infrared transmission [6] and synchrotron x rays [7,8].

The displacement of the condensed electrons in the strained CDW causes an elastic force that is opposite the applied field. In transport measurements, this opposite force must be overcome, leading to an additional voltage between the current contacts. This phase-slip voltage V_{PS} has been extensively studied for bulk crystals [9–13]. V_{PS} depends only weakly on the charge-density-wave current I_{CDW}, but increases strongly when temperature is lowered. Measurements on $NbSe_3$ crystals have shown that V_{PS} is length independent for spacings larger than 20 μm [12]. First experiments on antidot arrays [14], however, have provided an indication that the conversion mechanism changes at submicron length scales.

In this paper, we report the controlled study of phase slip on a mesoscopic scale. The measurements have been performed on small wires that were lithographically patterned into a $NbSe_3$ crystal. By changing contact pairs for current injection, the phase-slip voltage V_{PS} has been determined as a function of current-contact spacing. A significant reduction of V_{PS} is found for spacings smaller than 3 μm. We suggest that this reduction is a mesoscopic effect, related to the addition or removal of single CDW wave fronts.

The patterning of $NbSe_3$ crystals is discussed in detail elsewhere [15]. A thin crystal (thickness $d = 0.35$ μm), with a length of 4 mm (along the crystallographic b axis) and a width of 27 μm (along c), is glued to a sapphire substrate. An aluminum etch mask is then defined on top by the use of electron-beam lithography. Etching of the crystal occurs with an SF_6 plasma. In a second step, Au contacts are fabricated by near-UV optical lithography.

A typical $NbSe_3$ wire structure is shown in Fig. 1. The narrow part of the wire has a width (W) of 0.5 μm and a length of 40 μm. Instead of directly contacting the wire by gold probes, we have patterned 0.5μm wide voltage probes at the sides of the wire, within the $NbSe_3$ crystal. An advantage of this layout is the negligible shunting of current through the voltage probes. At the ends of the wire, 27×50 μm^2 large current pads are defined. Gold contacts connect to all eight terminals. Measurements have been performed on this wire, as well as on a similar wire with a width of 1 μm.

The room-temperature resistivity of the wires is 0.2 mΩ cm, which is comparable to values for unpatterned crystals [16]. Measurements with various combinations of voltage contacts show that this resistivity is constant throughout the wire. Peierls transitions occur at $T_{P1} = 58$ K and $T_{P2} = 142$ K. The resistance ratio $R(295\text{ K})/R(5\text{ K})$ is 14 for the 0.5 μm wide wire, and 25 for the 1 μm wide wire. These ratios are lower than those for thick $NbSe_3$ crystals, but they compare well with values for thin unpatterned $NbSe_3$ crystals of comparable thickness [17]. Clear Shapiro steps in the current-voltage [$I(V)$] characteristics show that sliding CDWs can be completely locked by an external ac signal. All these

 0031-9007/00/84(3)/538(4)$15.00

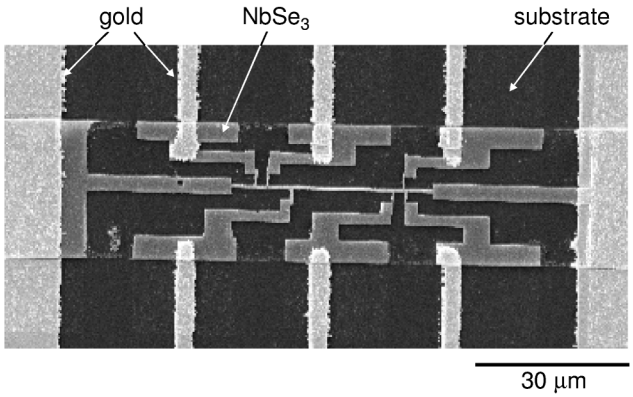

FIG. 1. Electron-microscope image of an eight-terminal $NbSe_3$ wire structure. The wire has a width of 0.5 μm. Voltage probes have been patterned into the crystal at mutual spacings of 2, 5, 20, 2, and 0.5 μm (from left to right; spacings are defined between the middles of the 0.5 μm wide ends of the probes). Large current pads are defined at both sides. The structure is electrically connected by Au contact probes.

measurements show that our electron-beam patterning process does not degrade the $NbSe_3$.

To determine the phase-slip voltage, we use the method introduced by Gill [18]. Transposed and normal four-terminal measurements are performed for a pair of contacts (see inset of Fig. 2). In the normal measurement, current is injected at the current pads, and current conversion occurs far away from the voltage probes. For the transposed configuration, on the other hand, current is injected through the middle probes, and conversion must occur in the small wire segment between the two probes. An additional voltage V_{PS} is measured in this configuration. When the voltages measured in normal and transposed configuration are plotted versus I_{CDW}, the voltage difference at fixed I_{CDW} is a measure for V_{PS}.

$I(V)$ characteristics are recorded by slowly ($\sim$1 mHz) sweeping the current and measuring the resulting voltage between a pair of contacts. The CDW current I_{CDW} is numerically determined from $I_{\mathrm{CDW}} = I - V/R$, where R is the resistance at small electric fields, when the CDW is pinned. We always find the same R (within tenths of a percent) for the transposed and the normal measurements. Some heating effects are observed for temperatures ranging from 70–90 K and for $T < 30$ K. Here, we present the data for temperatures between 100 and 140 K, where heating is absent.

Figure 2 shows typical $I_{\mathrm{CDW}}(V)$ characteristics in the normal and the transposed configuration. An increase of I_{CDW} is observed beyond a well-defined threshold voltage. For the normal measurement, the onset of sliding-CDW transport occurs at $V_T = 0.24$ mV, corresponding to a threshold field $E_T = 1.2$ V/cm. The value of E_T is independent of contact spacing, and compares well with typical values found for $NbSe_3$ crystals of similar thickness [17]. For the transposed configuration, nonzero I_{CDW} is observed for voltages larger than 1 mV. The difference between the curves is consistent with an additional

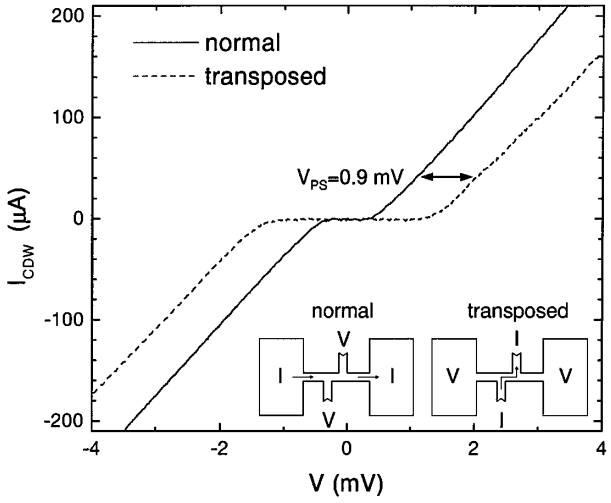

FIG. 2. Charge-density-wave current versus voltage for 2 μm spaced contacts on the 1 μm wide wire (120 K). The solid line denotes a measurement in the normal configuration, whereas the dashed line represents data for the transposed configuration (see inset). The phase-slip voltage V_{PS} is determined by subtracting the voltages for both curves at the same I_{CDW}.

phase-slip voltage required in the transposed configuration. At $I_{\mathrm{CDW}} = 40$ μA, we find $V_{\mathrm{PS}} = 0.9$ mV.

Remarkably, our data indicate that current conversion is complete for all contact spacings. In Fig. 2 transposed and normal $I_{\mathrm{CDW}}(V)$ curves nearly run parallel at high bias currents. Such parallel curves are found for all spacings. If current conversion had been incomplete, the $I_{\mathrm{CDW}}(V)$ curve for the transposed configuration would have been less nonlinear, and a strong increase of V_{PS} as a function of I_{CDW} would have been measured.

The clear difference between curves measured in transposed and normal configurations allows an accurate determination of V_{PS}. In Fig. 3a we plot V_{PS} vs the CDW current density j_{CDW}. Above a threshold phase-slip voltage, V_{PS} changes only slightly with increasing j_{CDW}. This typical dependence of V_{PS} on j_{CDW} is found for all temperatures and contact spacings. The measured phase-slip voltage at any j_{CDW} is more than a factor of 2 smaller for the 0.5 μm spaced contacts than for the 7 μm spaced contacts. This strong decrease of V_{PS} for small spacings is observed at all temperatures.

Figure 3b shows the temperature dependence of the phase-slip voltage. V_{PS} can be well fitted with an exponential function $V_{\mathrm{PS}} = V_{\mathrm{PS}}(0)e^{-T/T_0}$ in the range of temperatures studied. For T_0, we find values in the range 15–30 K. No systematic dependence of T_0 on L is found.

The central result of this paper is the reduction of V_{PS} for $L < 3$ μm. In Fig. 4b, V_{PS} has been plotted versus contact spacing for two temperatures. V_{PS} appears to be independent of wire width, as is evident from comparing data for the 0.5 and 1 μm wide wire. The V_{PS} values for the 5 and 7 μm spacings are in good agreement with values found for unpatterned bulk crystals [12]. Between 3 and 0.5 μm, however, V_{PS} decreases by a factor of 2 to 3. The curves in Fig. 4b are fits to $V_{\mathrm{PS}}(L) = LV_{\mathrm{PS}}(\infty)/(L_0 +$

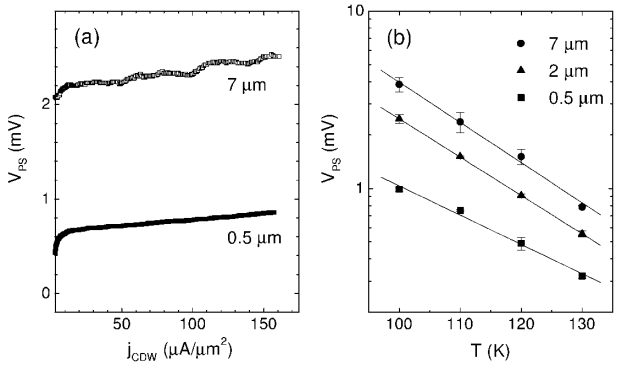

FIG. 3. (a) Phase-slip voltage versus charge-density-wave current density at 110 K for 0.5 and 7 μm spaced contacts. At any value of j_{CDW}, V_{PS} is more than a factor of 2 smaller for the 0.5 μm spaced contacts. (b) Temperature dependence of V_{PS} for three contact spacings. The curves are fits using $V_{\mathrm{PS}} = V_{\mathrm{PS}}(0)e^{-T/T_0}$, with $T_0 = 19$, 21, and 26 K for the 7, 2, and 0.5 μm spaced contacts, respectively.

L), where the characteristic length scale, $L_0 = 1.2$ μm at 120 K and 2.0 μm at 100 K.

At first sight, the observed reduction of V_{PS} may not be surprising. One could argue that in the transposed configuration on small length scales, geometrical effects may lower the nonlinear CDW conductivity (σ_{CDW}) or that current conversion is incomplete. However, our data clearly exclude both possibilities. We have not observed a decrease of σ_{CDW} as illustrated in Fig. 4a. In this figure σ_{CDW} is constant and does not show the pronounced size effect of V_{PS} in Fig. 4b [19]. Incomplete current conversion can also be ruled out. As shown above, $I_{\mathrm{CDW}}(V)$ curves do not show signs of incomplete conversion. Moreover, incomplete current conversion leads to an opposite trend for the length dependence of V_{PS}. Since the data in Fig. 4b at, for instance, 120 K are taken at the same j_{CDW}, the rate at which wave fronts are added (removed) is the same. To obtain the same j_{CDW}, incomplete conversion requires more strain. A *higher* V_{PS} would then be expected, contrary to the experimental observation. We will now compare our data with existing models for CDW current conversion.

A quantitative description of current conversion in CDW conductors has been given by Ramakrishna *et al.* [20]. In their model, strain caused by motion of CDW wave fronts lowers the energy barrier for thermal nucleation of phase-slip centers. The phase-slip rate critically depends on the strain, and current conversion occurs in a region near the contacts of length L_{PS} where the strain exceeds a critical value. V_{PS} is an experimental measure of the strain at the contacts. The model predicts that the strain depends linearly on the distance to the current contacts. When L is reduced, the strain profile is steeper. For fixed V_{PS}, the region in which phase-slip processes occur is smaller and hence the CDW current decreases. More strain and correspondingly a higher V_{PS} is therefore required to produce the same CDW current. Thus, in this model, V_{PS} increases as L decreases, in contradiction to our observations.

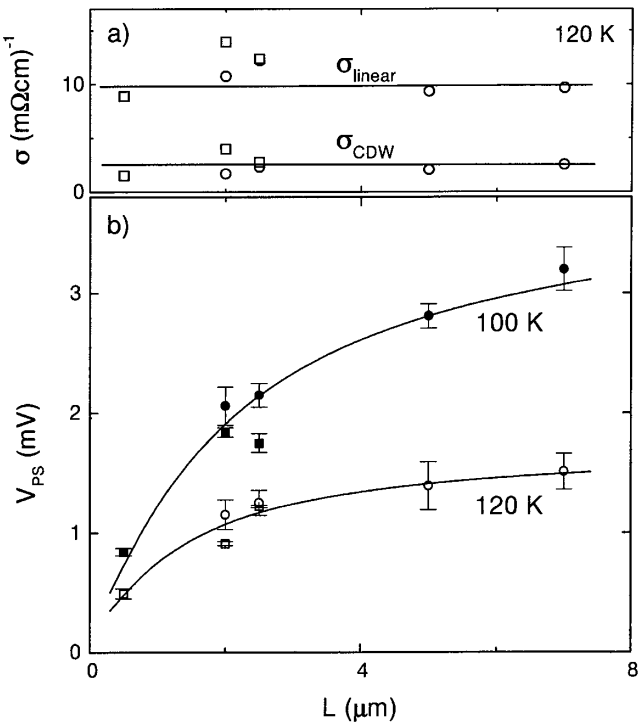

FIG. 4. (a) Low-bias conductivity (upper set of points) and the nonlinear CDW conductivity (lower set of points) vs contact spacing L, showing no sign of a finite size effect [19]. Data are taken at 120 K from curves measured in the transposed configuration. σ_{CDW} has been determined at $(E - E_T) = 5$ V/cm and multiplied by a factor of 3. Horizontal lines are guides to the eye. Circles: 0.5 μm wide wire; squares: 1 μm wide wire. (b) Phase-slip voltage V_{PS} vs L taken at $j_{\mathrm{CDW}} = 57$ μA/μm^2 (120 K) and $j_{\mathrm{CDW}} = 0$ μA/μm^2 (100 K). A strong decrease of V_{PS} is seen at low L. Circles: 0.5 μm wide wire; squares: 1 μm wide wire. Error bars denote the (nonsystematic) difference between positive and negative current. Curves are fits to $V_{\mathrm{PS}}(L) = LV_{\mathrm{PS}}(\infty)/(L_0 + L)$ with $L_0 = 1.2$ μm for the data taken at 120 K and 2 μm for the data at 100 K.

For small contact spacings, phase-slip processes beyond the current contacts [12,21] have to be taken into account. This is particularly important in samples where the distance, over which the strain profile extends beyond the contacts ($\approx V_{\mathrm{PS}}/2E_T$), exceeds L. In that case, most phase-slip events occur beyond the contacts and one expects [22] V_{PS} to be practically independent of L. We have performed computer simulations based on the work in Ref. [21], which have confirmed this picture. Our samples are in the limit $V_{\mathrm{PS}}/2E_T > L$ but the observation of a length dependent V_{PS} disagrees with this model.

Another consequence of phase-slip processes beyond the contacts is that they lower the measured V_{PS} [21]. Outside the current contacts, no net current can exist, and a backflow of normal electrons compensates the CDW current that flows here. This backflow current causes an opposite voltage and therefore decreases the measured V_{PS}. At most, this correction factor is RI_{CDW}. Here, $R = \rho_N L_{\mathrm{PS}}/Wd$ with ρ_N the resistivity of the uncondensed electrons. An upper limit for L_{PS} can be obtained by measuring voltages beyond the current contacts.

We find [23] that $L_{PS} < 2\ \mu$m, so that for the data of Fig. 4b the correction factor is smaller than 0.1 mV. We therefore conclude that phase-slip processes beyond the contacts cannot explain our experimental data.

We suggest that the reduction of V_{PS} is a mesoscopic effect, associated with the small dimensions of our sample. For bulk crystals, the number of wave fronts between the current contacts is large. Adding a single wave front will therefore not significantly change the macroscopic strain profile. At micrometer length scales, however, the situation is different. For a $NbSe_3$ wire with a length of 3 μm, there are about 2000 CDW wave fronts between the current contacts ($\lambda_{CDW} \approx 1.4$ nm). X-ray studies have shown [7,8] that the typical change of the CDW wavelength as a result of strain is about 0.1% [24]. This means that in the 3 μm long wire only one additional wave front is accommodated in the compressed CDW and similarly one wave front is missing in the stretched CDW. If, in this situation, one single wave front is removed or added, the strain profile will be dramatically changed [25].

At this moment, it is unclear how the phase-slip process proceeds in mesoscopic samples. Events at both contacts may occur in an uncorrelated way. After a phase-slip event, the sliding-CDW motion restores the strain until a new phase slip takes place. On average, there will be less strain and the measured, time-averaged V_{PS} is reduced. On the other hand, phase-slip events may become correlated in coherent samples: addition of a wave front at one contact then runs synchronously with the removal of a wave front at the other contact. Coherent phase slip requires less deformation of the CDW. As a result there is less strain and the measured phase-slip voltage is reduced compared to its bulk value.

We acknowledge Serge Lemay for discussions and sharing his computer code of the model in Ref. [21], Gerrit Bauer for discussions, E. Slot for the simulations, and Arjan Kalwij for his assistance with the measurements. This work was supported by the Netherlands Foundation for Fundamental Research on Matter (FOM). H. S. J. v. d. Z. was supported by the Dutch Royal Academy of Arts and Sciences (KNAW). Yu. I. L. acknowledges support through RFBR Grant No. 99-02-17364.

[1] For reviews on CDWs, see G. Grüner, *Density Waves in Solids* (Addison-Wesley Publishing Company, Reading, MA, 1994); *Physics and Chemistry of Low-Dimensional Inorganic Conductors*, edited by C. Schlenker, J. Dumas, M. Greenblatt, and S. van Smaalen (Plenum, New York, 1996).

[2] J. S. Langer and V. Ambegaokar, Phys. Rev. **164**, 498 (1967).

[3] J. S. Langer and M. E. Fisher, Phys. Rev. Lett. **19**, 560 (1967).

[4] L. P. Gor'kov, JETP Lett. **38**, 87 (1983).

[5] N. P. Ong and K. Maki, Phys. Rev. B **32**, 6582 (1985).

[6] M. E. Itkis, B. M. Emerling, and J. W. Brill, Phys. Rev. B **52**, R11 545 (1995).

[7] D. DiCarlo, E. Sweetland, M. Sutton, J. D. Brock, and R. E. Thorne, Phys. Rev. Lett. **70**, 845 (1993).

[8] H. Requardt, F. Ya. Nad', P. Monceau, R. Currat, J. E. Lorenzo, S. Brazovskii, N. Kirova, G. Grübel, and Ch. Vettier, Phys. Rev. Lett. **80**, 5631 (1998).

[9] J. C. Gill, Physica (Amsterdam) **143B**, 49 (1986).

[10] D. V. Borodin, S. V. Zaitsev-Zotov, and F. Ya. Nad', Sov. Phys. JETP **66**, 793 (1987).

[11] J. C. Gill, Phys. Rev. Lett. **70**, 331 (1993).

[12] M. P. Maher, T. L. Adelman, D. A. DiCarlo, J. P. McCarten, and R. E. Thorne, Phys. Rev. B **52**, 13 850 (1995).

[13] S. G. Lemay, M. C. de Lind van Wijngaarden, T. L. Adelman, and R. E. Thorne, Phys. Rev. B **57**, 12 781 (1998).

[14] Yu. I. Latyshev, B. Pannetier, and P. Monceau, Eur. Phys. J. B **3**, 421 (1998).

[15] O. C. Mantel, F. Chalin, C. Dekker, H. S. J. van der Zant, Yu. I. Latyshev, B. Pannetier, and P. Monceau, Synth. Met. **103**, 2612 (1999).

[16] P. Monceau, J. Richard, and M. Renard, Phys. Rev. B **25**, 931 (1982).

[17] J. McCarten, D. A. DiCarlo, M. P. Maher, T. L. Adelman, and R. E. Thorne, Phys. Rev. B **46**, 4456 (1992).

[18] J. C. Gill, Solid State Commun. **44**, 1041 (1982).

[19] The scatter in σ_{CDW} correlates with variations in σ_0. All σ_{CDW} data can be mapped on the lower horizontal line in Fig. 4a when using an effective contact spacing determined from the σ_0 data or from the threshold field data of the normal four-probe configuration. A length independent σ_0 or E_T yields calculated lengths that are within $0.1-0.4\ \mu$m of the defined spacings.

[20] S. Ramakrishna, M. P. Maher, V. Ambegaokar, and U. Eckern, Phys. Rev. Lett. **68**, 2066 (1992); S. Ramakrishna, Phys. Rev. B **48**, 5025 (1993).

[21] T. L. Adelman, M. C. de Lind van Wijngaarden, S. V. Zaitsev-Zotov, D. DiCarlo, and R. E. Thorne, Phys. Rev. B **53**, 1833 (1996).

[22] Note that the model of Refs. [12,21] has been developed to describe bulk samples with local pinning as is appropriate over distances large compared with the Lee-Rice phase-coherence length. Its application may become questionable for samples with mesoscopic sizes.

[23] We found that the voltage drop beyond a distance of 2 μm from the current contact is reduced to 2% or less from the voltage drop between the current probes. This measurement indicates that $L_{PS} < 2\ \mu$m, a value that is consistent with values estimated from our computer simulations.

[24] The x-ray data [7,8] for the strain amplitude are for $T = 90$ K. At the higher temperatures of our measurements, the strain amplitude will be smaller. In this case, less than one extra wave front can be accommodated.

[25] We believe that the length $(V_{PS}/2E_T)$ over which the strain profile extends beyond the contacts does not determine its relaxation. Beyond the contacts, the pinning force is balanced by the elastic force so that a large energy (corresponding to twice the pinning field) is needed for wave fronts to start moving. This picture is consistent with Fig. 14 of Ref. [21], which shows that relaxation initially occurs over a length L_{PS}. In our samples, L_{PS} is small and the contact spacing is the important length scale determining this process.